Supporting Information

Realistic multidimensional opto-electrical modeling guide for CIGSe solar cells

Jan Lucaßen[1], *Setareh Sedaghat*[1], *Martina Schmid**

[1] Co-first authors

Absorption in CIGSe

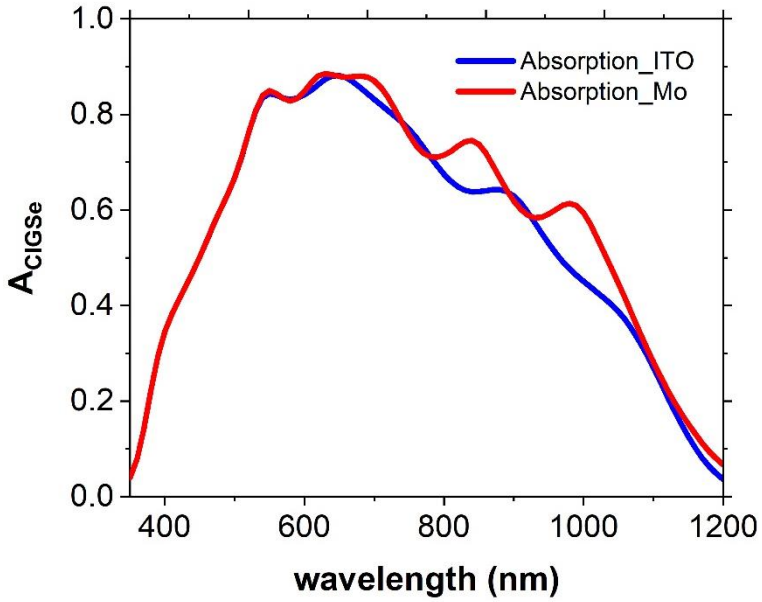

Figure S1: The CIGSe absorption on Mo (red line) and ITO (blue line)

Figure S1 shows the CIGSe absorption A_{CIGSe} grown on two different back contacts Mo and ITO. For CIGSe solar cells on Mo, A_{CIGSe} (red line) reaches a maximum value of 89% at 690 nm wavelength and then incomplete absorption leads to a drop in A_{CIGSe} for longer wavelengths.

This reduction at longer wavelengths can be correlated with poor reflectivity and parasitic absorption of Mo. Furthermore, a simulated CIGSe solar cell on ITO back contact shows a A_{CIGSe} maximum value of 87% at 650 nm wavelength (blue line). For longer wavelengths, the reduced A_{CIGSe} leads to increased transmission.

Work functions of the back contacts

Table S1: Work function of Mo for different crystal orientations.

Crystal Orientation	Work Function ϕ_m (eV)
	4.6
(100)	4.53
(110)	4.95
(111)	4.55
(112)	4.36
(114)	4.5
(332)	4.55

The work function ϕ_m of molybdenum depends on its crystal orientation, as summarized in Table S1.[1] Different treatments like annealing or etching can still alter the work function. We can adapt the work function in the simulations to fit our experimental Mo properties.
For ITO, the work function is also dependent on different treatment as well as on the measurement method. Table S2 indicates the measured values for ITO according to different literature.

Table S2: Work function of ITO derived for different treatments and measurement approaches.

Treatment	Measurement	Work Function ϕ_m (eV)
Heating [2]	UPS*	4.47-4.48
Ar ion Sputtering [2]	UPS	4.42-4.48
Chemical Cleaning [3]	XPS‡ prior to UPS UPS XPS after UPS	4.78 4.2 4.17
Oxygen Plasma [3]	XPS prior to UPS UPS XPS after UPS	5.24 4.85 4.89
Untreated [3]	XPS prior to UPS UPS XPS after UPS	4.26 4.25 4.28
Untreated [4]	Cyclic Voltammetry Technique	4.49-4.65

*UPS: Ultraviolet Photoemission Spectroscopy, ‡XPS: X-ray Photoemission Spectroscopy

Surface Recombination Velocity

Since the thermionic emission is generally assumed to be one source of current transport in Schottky contacts besides the thermionic diffusion, the surface recombination velocities for electrons and holes (S_{bn} and S_{bp}) are calculated by thermionic emission theory (for details see ref. [5]):

$$\boldsymbol{S_{bn} = \frac{A_n^* T^2}{q N_c}} \tag{1a}$$

$$\boldsymbol{S_{bp} = \frac{A_p^* T^2}{q N_v}} \tag{1b}$$

where q is the elemental charge, T the temperature, N_c and N_v are the densities of states in the conduction and valence band, respectively, and $\boldsymbol{A_n^*}$ and $\boldsymbol{A_p^*}$ are the effective Richardson constants for electron and holes.

The effective Richardson constants for electrons and holes by ignoring quantum-mechanical tunneling and phonon scattering are given by:

$$\boldsymbol{A_n^* = \frac{4\pi q m_e^* k_B^2}{h^3}} \tag{2a}$$

$$\boldsymbol{A_p^* = \frac{4\pi q m_h^* k_B^2}{h^3}} \tag{2b}$$

where h is Plank's constant, and $\boldsymbol{m_e^*}$ and $\boldsymbol{m_h^*}$ are the effective masses of electrons and holes in CIGSe. The effective masses for electrons and holes in CIGSe are $0.1\,\boldsymbol{m}^*$ and $0.3\,\boldsymbol{m}^*$, respectively, where $\boldsymbol{m}^*$is the effective mass of the free electron [6].

Defects in CIGSe

Chalcopyrites, like copper indium gallium diselenide ($Cu(In,Ga)Se_2$ or short CIGSe), are multi-crystalline compound semiconductors with a double zinc blende lattice structure, as shown in Figure S2.

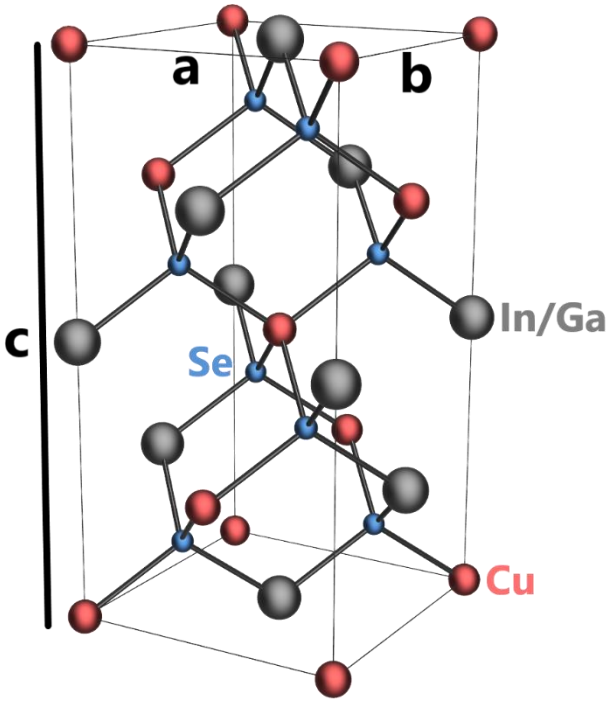

Figure S2: Crystal Lattice of CIGSe

Because of its multi-crystalline nature, many crystal defect types are possible. These will act as p- or n-type doping. Zhang et al. calculated the defect formation energies of all potential defects in the $CuInSe_2$ structure and concluded that Cu vacancies need the lowest formation energy for most growth conditions and are thus dominant.[7] For the growth conditions corresponding to our experimental cells (Cu-poor and In-rich with a p-type absorber), Zhang et al. derived a list of the most common defects, including vacancies ($V_{missing\text{-}element}$), i.e., missing elements in the lattice, interstitials ($Element_i$), i.e. elements in between the lattice positions and antisites ($Element_{replaced\text{-}element}$), i.e. an element replacing another one. In this naming, the most abundant defects can be ranked by their formation energy according to $V_{Cu} < In_{Cu} < V_{In} < Cu_{In} < Cu_i$. For the CIGSe absorber, gallium-type formations are also possible and will have a similar effect as the indium formations. Selenium formations are also quite common but were not accounted for in the ranking.

In the absorber structure, the Cu vacancies will act as a shallow acceptor defect giving the absorber its p-type nature, while the In/Ga_{Cu}-antisites will serve as deep donor defects.[7-9] These two defects ($2V_{Cu} + In_{Cu}$) can form a stable charge-neutral defect complex called Ordered Defect Compound (ODC), which will naturally form on the surface of the absorber. [10]

The experimental samples used for verifying our model were grown with sodium supply to improve the electrical properties.[11] Wei et al. looked into the effect of sodium in the $CuInSe_2$ absorber and concluded that sodium will reduce the In_{Cu} defects breaking the ODC.[9]

When trying different cell stacks and parameters in COMSOL, defects showed a specific behavior which should be clarified here. In COMSOL, there are four different types of traps: donor traps with a positive charge when unoccupied and neutral hole traps with a positive charge when occupied, as well as acceptor traps with a negative charge when unoccupied, and neutral electron traps with a negative charge when occupied (in the other cases, the traps are

then neutral) [12]. In Figure S3, the different trap types are illustrated, and their charge states when un-/occupied. E_g is the semiconductor's bandgap, E_C is the conduction band minimum, E_{Fn} is the electron Fermi-level, E_{Fp} is the hole Fermi-level, and E_V is the valence band maximum.

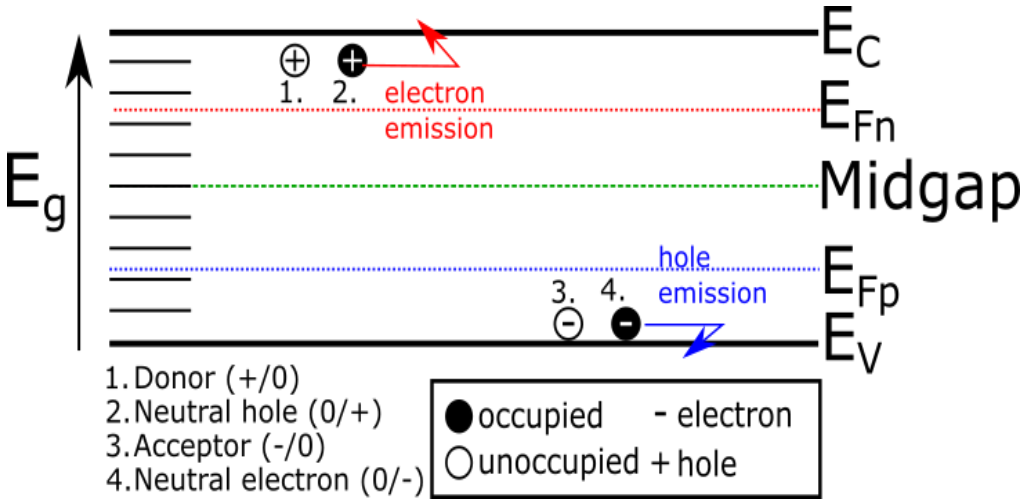

Figure S3: Typical trap types in Comsol and their corresponding state of occupation (unoccupied/ occupied) according to their positions in the bandgap.

Donor traps have mostly energy levels above midgap, while acceptor traps have energy levels below midgap [7]. A transition energy level gives the energetic position of the trap inside the bandgap and the most likely state of occupation depending on the position of the transition energy level compared to the Fermi level. Donor traps in a p-type layer in COMSOL are mostly unoccupied when close to the conduction band minimum (E_C) and above the electron Fermi level because the probability of an electron being captured from the valence band is less than 50%, above the electron Fermi level. If the traps remain unoccupied, their charge influences the band diagram, and they stay active as a recombination center. In addition, acceptor traps will be mostly unoccupied when close to the valence band maximum (E_V) and below the hole Fermi level because in equilibrium the probability of holes being captured from the valence band is lower than 50%.

Moreover, all processes are defined for electrons, i.e., an electron emission (ee) can be described as an electron being emitted from the trap level to the conduction band, and the electron capture (ec) can be described as an electron being captured from the conduction band into the trap level. The hole emission (he) can be described as an electron being excited from the valence band into the trap state [13]. The hole capture (hc) is described as an electron moving from the trap into a free state in the valence band. These four mechanisms are used to describe all trap-related interactions.

The influence of the different trap types in COMSOL is dependent on the doping type of the layer they are applied to. If the layer is p-type, acceptor traps and neutral electron traps will have the same effect and be most influential. However, if the layer is n-type, the donor traps and neutral hole traps act comparably and are most influential. The traps' influence is mainly caused by their respective charges, when occupied/ unoccupied and not by recombination specifically.

The crystal defect counterpart for the trap is essential for applying realistic traps. The possible defects in CIGSe and their corresponding trap types are clarified in Table S3.

Table S3: Table of crystal defects in CIGSe and corresponding traps with their charge states unoccupied/occupied for acceptor and donor trap and occupied/unoccupied for neutral traps.

Element (Ion Charge)	Vacancy (Opposite of Ion Charge)	Interstitial (Ion Charge)	Antisite at Cu (V_{Cu}^{-1}+ Ion)	Antisite at In/Ga ($V_{In/Ga}^{-3}$ + Ion)	Antisite at Se (V_{Se}^{+2} + Ion)
Copper ($^{+1}$)	Acceptor trap ($^{-1}$)/ Neutral Electron Trap (-/0)	Donor trap ($^{+1}$)/ Neutral Hole Trap (+/0)	-	Acceptor trap ($^{-2}$)/ Neutral Electron Trap (-/0)	Donor trap ($^{+3}$)/ Neutral Hole Trap (+/0)
Indium ($^{+3}$)	Acceptor trap ($^{-3}$)/ Neutral Electron Trap (-/0)	Donor trap ($^{+3}$)/ Neutral Hole Trap (+/0)	Donor trap ($^{+2}$)/ Neutral Hole Trap (+/0)	-	Donor trap ($^{+5}$)/ Neutral Hole Trap (+/0)
Gallium ($^{+3}$)	Acceptor trap ($^{-3}$)/ Neutral Electron Trap (-/0)	Donor trap ($^{+3}$)/ Neutral Hole Trap (+/0)	Donor trap ($^{+2}$)/ Neutral Hole Trap (+/0)	-	Donor trap ($^{+5}$)/ Neutral Hole Trap (+/0)
Selenium ($^{-2}$)	Donor trap ($^{+2}$)/ Neutral Hole Trap (+/0)	Acceptor trap ($^{-2}$)/ Neutral Electron Trap (-/0)	Acceptor trap ($^{-3}$)/ Neutral Electron Trap (-/0)	Acceptor trap ($^{-3}$)/ Neutral Electron Trap (-/0)	-
Sodium ($^{+1}$)	-	Donor trap ($^{+1}$)/ Neutral Hole Trap (+/0)	Neutral	Acceptor trap ($^{-2}$)/ Neutral Electron Trap (-/0)	Donor trap ($^{+3}$)/ Neutral Hole Trap (+/0)
Cadmium ($^{+2}$)	-	Donor trap ($^{+2}$)/ Neutral Hole Trap (+/0)	Donor trap ($^{+1}$)/ Neutral Hole Trap (+/0)	Acceptor trap ($^{-1}$)/ Neutral Electron Trap (-/0)	Donor trap ($^{+4}$)/ Neutral Hole Trap (+/0)

In addition to the elements of the absorber itself and incorporated sodium, Cd will diffuse into the absorber when depositing the buffer layer of CdS. Kiss et al. showed theoretically that Cd could diffuse into the top parts of the absorber layer forming Cd_{Cu} - antisites and modifying the surface to become n-type [14]. Nakada et al. showed direct evidence that CdS will diffuse into the absorber during chemical bath deposition [15]. Due to the Cd diffusion, a thin n-type interface layer was applied in the simulations together with donor traps to account for the impurities/defects at the interface between CdS and absorber.

Furthermore, acceptor traps were added inside the absorber layer with a Gaussian distribution towards the back of the absorber representing an increasing amount of Cu-vacancies and Se as antisite on the other element positions or as interstitial towards the back contact. The sodium will cancel the Se antisites and Cu vacancies at the back of the absorber and reduce or stop a rollover from happening. The reduction of acceptor trap density or width of Gaussian distribution will model an increase in sodium doping. Interface states are used at the back contact to account for $MoSe_2$ or GaO_x, which are likely formed during the absorber growth on Mo or ITO back contact, respectively. These interface states were added in addition to the traps.

[1] H. B. Michaelson, "The work function of the elements and its periodicity," *J.Appl.Phys.*, vol. 48, no. 11, pp. 4729-4733, 1977/11/01 1977, doi: 10.1063/1.323539.
[2] Y. Park, V. Choong, Y. Gao, B. R. Hsieh, and C. W. Tang, "Work function of indium tin oxide transparent conductor measured by photoelectron spectroscopy," *Applied Physics Letters*, vol. 68, no. 19, pp. 2699-2701, 1996/05/06 1996, doi: 10.1063/1.116313.
[3] R. Schlaf, H. Murata, and Z. H. Kafafi, "Work function measurements on indium tin oxide films," *Journal of Electron Spectroscopy and Related Phenomena*, vol. 120, no. 1, pp. 149-154, 2001/10/01/ 2001, doi: https://doi.org/10.1016/S0368-2048(01)00310-3.
[4] H. D. Kwak, D. S. Choi, Y. K. Kim, and B. C. Sohn, "Study on the work function of various ITO substrates using electrochemical analysis," *Molecular Crystals and Liquid Crystals Science and Technology. Section A. Molecular Crystals and Liquid Crystals*, vol. 370, no. 1, pp. 47-52, 2001/10/01 2001, doi: 10.1080/10587250108030036.
[5] S. M. Sze and K. N. Kwok, *Physics of semiconductor devices*. Hoboken, New Jersey. Published simutaneously in Canada: John Wiley & Sons, 2007.
[6] C. Persson, "Anisotropic hole-mass tensor of $CuIn_{1-x}Ga_x(S,Se)_2$: Presence of free carriers narrows the energy gap," *Applied Physics Letters*, vol. 93, no. 7, p. 072106, 2008, doi: 10.1063/1.2969467.
[7] S. B. Zhang, S.-H. Wei, A. Zunger, and H. Katayama-Yoshida, "Defect physics of the $CuInSe_2$ chalcopyrite semiconductor," *Physical Review B*, vol. 57, no. 16, pp. 9642-9656, 04/15/ 1998, doi: 10.1103/PhysRevB.57.9642.
[8] S. Siebentritt, M. Igalson, C. Persson, and S. Lany, "The electronic structure of chalcopyrites—bands, point defects and grain boundaries," *Progress in Photovoltaics: Research and Applications*, vol. 18, no. 6, pp. 390-410, 2010, doi: https://doi.org/10.1002/pip.936.
[9] S.-H. Wei, S. B. Zhang, and A. Zunger, "Effects of Na on the electrical and structural properties of $CuInSe_2$," *J.Appl.Phys.*, vol. 85, no. 10, pp. 7214-7218, 1999, doi: 10.1063/1.370534.
[10] A. Niemegeers, M. Burgelman, R. Herberholz, U. Rau, D. Hariskos, and H. W. Schock, "Model for electronic transport in $Cu(In,Ga)Se_2$ solar cells," *Progress in Photovoltaics: Research and Applications*, standard vol. 6, pp. 407-421, 1998.
[11] Y. Li, G. Yin, Y. Gao, T. Köhler, J. Lucaßen, and M. Schmid, "Sodium control in ultrathin $Cu(In,Ga)Se_2$ solar cells on transparent back contact for efficiencies beyond 12%," *Solar Energy Materials and Solar Cells*, vol. 223, p. 110969, 2021/05/01/ 2021, doi: https://doi.org/10.1016/j.solmat.2021.110969.
[12] C. Multiphysics, "Semiconductor module user's guide," https://doc.comsol.com/5.3/doc/com.comsol.help.semicond/SemiconductorModuleUsersGuide.pdf, 2017. [Online]. Available: https://doc.comsol.com/5.3/doc/com.comsol.help.semicond/SemiconductorModuleUsersGuide.pdf
[13] Comsol Group. "COMSOL Multiphysics." https://www.comsol.com/ (accessed.
[14] J. Kiss, T. Gruhn, G. Roma, and C. Felser, "Theoretical study on the diffusion mechanism of Cd in the Cu-poor phase of CuInSe2 solar cell material," *The Journal of Physical Chemistry C*, vol. 117, no. 49, pp. 25933-25938, 2013/12/12 2013, doi: 10.1021/jp4087877.
[15] T. Nakada and A. Kunioka, "Direct evidence of Cd diffusion into Cu,In,Ga,Se_2 thin films during chemical-bath deposition process of CdS film," *Applied Physics Letters*, standard vol. 74, no. 17, pp. 2444-2446, 26.04.1999 1999.